RSC Advances

ROYAL SOCIETY OF CHEMISTRY

www.rsc.org/advances

Graphical Abstract

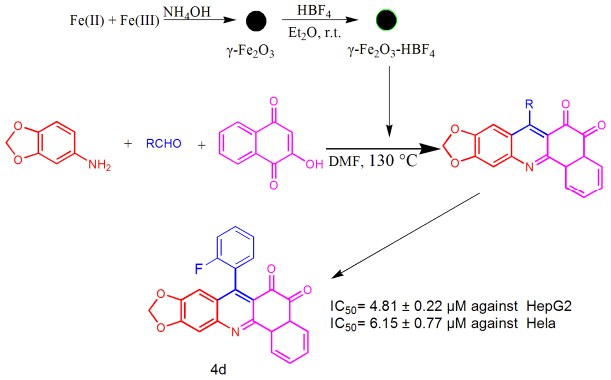

Nano γ-Fe_2O_3-supported fluoroboric acid as a novel magnetically catalyst was synthesized, and was used for efficient synthesis of synthesis of benzoacridinediones

Nano γ-Fe_2O_3-supported fluoroboric acid: a novel magnetically recyclable catalyst for the synthesis of 12-substituted-benzo[*h*][1,3]dioxolo[4,5-*b*] acridine-10,11-diones as potent antitumor agents

Xiaojuan Yang,[a] Chong Zhang,[b] Liqiang wu[b,*]

[a] *College of Chemistry and Chemical Engineering, Xinxiang University, Xinxiang, Henan 453003, China*

[b] *School of Pharmacy, Xinxiang Medical University, Xinxiang 453003, China*

ABSTRACT Nano γ-Fe_2O_3-supported fluoroboric acid as a novel magnetically catalyst was synthesized and characterized. The nanoparticle reagent was obtained with good loading levels and has been successfully used for efficient and selective synthesis of 12-substituted-benzo[*h*] [1,3]dioxolo[4,5-*b*]acridine-10,11-diones. The catalyst is quantitatively recovered by an external magnet and can be reused for six cycles with almost consistent activity. In addition, all the synthetic derivatives were fully characterized by spectral data and evaluated for their antitumor activity on human hepatoma cells (HepG2) and Henrietta Lacks strain of cancer cells (Hela), among the 19 new compounds screened, 12-(2-fluorophenyl)-benzo[*h*][1, 3]dioxolo[4,5-*b*]acridine-10,11-dione (**4d**) has pronounced activity.

Keywords: Nano γ-Fe_2O_3-supported fluoroboric acid; Aldehydes; *ortho*-Naphthoquinones; Heterogeneous catalysis; Antitumor; Multicomponent reactions

*Corresponding author. Tel.: +86 371 3029879; fax: +86 371 3029879; e-mail: wliq870@163.com

Introduction

Along with the living habits and environment changes, cancer has become the major cause of death in both developing and developed countries. Despite the efforts to discover and develop small molecule anticancer drugs in the last decade,[1] the development of new antitumor agents with improved tumor selectivity, efficiency, and safety remains desirable. Recently, naphthoquinones have been reported to posses diverse biological and therapeutic properties including antioxidant,[2] antifungal,[3] anti-inflammatory,[4] antiviral,[5] and anticancer activities.[6] Among these active compounds, 1,2-naphthoquinones include Tanshinone IIA,[7] 4-Hydroxysaprothoquinone,[8] β-Lapachone,[9] Mansonones[10] and Salvicine[11] (Figure 1) have been reported to show remarkable antitumor activities by means of inhibiting multiple enzymes. One of these quinones was Salvicine, a novel diterpenoid quinone compound, which possesses potent *in vitro* and *in vivo* activities against malignant tumor cells, especially in some human solid tumor models, and has now entered phase II clinical trials.[12] Salvicine induces apoptosis in various human tumor cell lines and displays prominent activity against multiple-drug resistance.[13] Mechanistic studies have shown that Topo II functions as one of the primary molecular targets of Salvicine.[14] These recent examples highlight the ongoing interest toward new 1,2-naphthoquinone derivatives and have prompted us to investigate this pharmacophore in drug discovery programs aiming at synthesizing novel bioactive molecules.

< Figure 1>

In recent years, magnetite or maghemite nanoparticles acquired organic chemists' attention as a new alternative to porous materials for supporting catalytic transformations.[15] The magnetic nature of these particles allows for easy recovery and recycling of the catalysts by an external magnetic field, which may handle operational cost and enhance product's purity. Moreover, magnetic nanoparticles can be functionalized easily through appropriate surface modifications, which are able to load various

functionalities.[16]

Multicomponent domino reactions have become an increasingly useful tool for the synthesis of chemically and biologically important benzoacridinediones because of their convergence, atom economy, and other suitable characteristics from the point of view of green chemistry.[17] As a continuation of our interest in developing efficient and environmental benign synthetic methodologies,[18] we report herein on the preparation of a new type of magnetically separable nano γ-Fe_2O_3-supported fluoroboric acid (γ-Fe_2O_3-HBF_4) and their application for the synthesis of 12-substituted-benzo[*h*][1,3]dioxolo[4,5-*b*] acridine-10,11-diones (Scheme 1) as potent antitumor agents.

< Scheme 1>

Results and Discussion

To prepare γ-Fe_2O_3-HBF_4, we have first chosen a known nano magnet γ-Fe_2O_3, which can be easily prepared by coprecipitation of ferrous (Fe^{2+}) and ferric (Fe^{3+}) ions in a basic aqueous solution followed by thermal treatment according to the reported procedure. Then, HBF_4 was added to a suspension of γ-Fe_2O_3 in Et_2O, while dispersed by sonication. The mixture was concentrated and the residue was heated at 100 °C for 72 h under vacuum to obtained nano γ-Fe_2O_3-supported fluoroboric acid (Scheme 2).

< Scheme 2>

The γ-Fe_2O_3-HBF_4 was characterized by FT-IR spectroscopy, energy dispersive spectroscopy (EDS), scanning electron microscopy (SEM), transmission electron microscopy (TEM), X-ray powder diffraction (XRD), vibrating sample magnetometer (VSM), thermogravimetric analysis (TGA) and elemental analysis. The specific surface area of the powders was determined by use of the BET method. Unfortunately, due to the magnetic properties of γ-Fe_2O_3-HBF_4 it is actually impossible to further

characterize this material by using solid state NMR spectroscopy.

Figure 2 shows FT-IR spectra for γ-Fe_2O_3 nanoparticles and γ-Fe_2O_3-HBF_4. The FT-IR spectra of nano γ-Fe_2O_3 exhibits two characteristic peaks at 562 cm^{-1} and 638 cm^{-1} due to the stretching vibrations of Fe-O bond in γ-Fe_2O_3. The FT-IR spectra of γ-Fe_2O_3-HBF_4 show Fe–O vibrations in the same vicinity. Compared with the unfunctionalized γ-Fe_2O_3 and the significant features observed for γ-Fe_2O_3-HBF_4 were the appearances of the peaks 1033 cm^{-1} (B–F stretching vibration). This analysis, in combination with microanalysis data (Figure 3), indicated the successful in loading of the HBF_4 groups onto the magnetic nanoparticles. The amount of HBF_4 loaded on the surface of nano γ-Fe_2O_3 was determined by TG analysis and confirmed by ion-exchange pH analysis.

< Figure 2>

< Figure 3>

The XRD pattern of γ-Fe_2O_3-HBF_4 shows characteristic peaks and relative intensity, which match well with the cubic structure of maghemite (JCPDS file No 39-1364). Diffraction peaks at around 30.32, 35.60, 43.30, 54.42, 57.20, 62.98 corresponding to the (220), (311), (400), (422), (511) and (440) faces are readily recognized from the XRD pattern (Figure 4). The average crystallitesize was calculated to be 13.4 nm using the Scherrer equation. The XRD combined with element analysis (B 0%, F %) of γ-Fe_2O_3-HBF_4 heated to 600°C display all F is lost as HF/HBF4 into the gas phase and Fe fluoride is not formed.

< Figure 4>

One indication of bond formation between the nanoparticles and the catalyst can be inferred from TGA. The TGA was also used to determine the percent of HBF_4 groups physisorbed onto the surface of magnetic nanoparticle. The TGA curve of the γ-Fe_2O_3-HBF_4 shows the mass loss of the HBF_4 group

as it decomposes upon heating (Figure 5). The weight loss at temperatures below 100 ˚C is due to the removal of physically adsorbed water. HBF_4 groups have been reported to desorb at temperatures above 160 ˚C. A weight loss about 6.6% from 160–500 ˚C, resulting from the removal of OH and HBF_4 hysisorbed onto the MNPs surface.

< Figure 5>

The shape and surface morphology of removal were investigated by SEM and TEM. As shown in Figure 6, The low magnification SEM images shows small nano sized grains having spherical and quasi spherical morphology with a narrow size distribution, which indicates the nano crystalline nature of γ-Fe_2O_3 nano particles. The presence of some larger particles attributes aggregating or overlapping of smaller particles. The sizes of removal are further analyzed by TEM and the results (Figure 7) showed the nano particles have nano dimension ranging from 10 to 20 nm. In TEM images, the shapes of are relatively rather rectangular, which is attributed to the presence of HBF_4 groups physisorbed onto the γ-Fe_2O_3 surfaces.

< Figure 6>

< Figure 7>

Superparamagnetic particles are beneficial for magnetic separation, the magnetic property of γ-Fe_2O_3 and γ-Fe_2O_3-HBF_4 were characterized by VSM. The room temperature magnetization curves of γ-Fe_2O_3 and γ-Fe_2O_3-HBF_4 are shown in Figure 8. As expected, the bare γ-Fe_2O_3, showed the higher magnetic value (saturation magnetization, Ms) of 61.4 emu/g, the Ms value of γ-Fe_2O_3-HBF_4 is decreased due to the increasing amount of nonmagnetic material on a particle surface makes a larger percentage of the particle mass nonmagnetic. However, this value is sufficiently high for magnetic separation. The strong magnetization of the nanoparticle was also revealed by simple attraction with an external magnet.

< Figure 8>

The N_2 adsorption–desorption isotherm provided a valuable tool for studying the textural and structure properties. The specific surface area of the powders was determined by use of the Brunauer–Emmett–Teller (BET) method. BET results showed that the average surface area of γ-Fe_2O_3 was 73.79 m^2g^{-1} and that of γ-Fe_2O_3-HBF_4 was 68.84 m^2g^{-1} (Figure 9). It was noted that γ-Fe_2O_3 had much higher surface area than γ-Fe_2O_3-HBF_4. This seems logical as the successful anchoring HBF_4 on the surface of MNP, decreasing the surface area.

< Figure 9>

The one-pot synthesis of 12-substituted-benzo[*h*] [1,3]dioxolo[4,5-*b*]acridine-10,11-diones **4** was achieved by the three-component condensation of 3,4-methylenedioxyaniline, aldehydes and 2-hydroxy -1,4-naphthoquinone in the presence of γ-Fe_2O_3-HBF_4 as a heterogeneous catalyst (Scheme 1). To find optimum conditions, the synthesis of 12-substituted-benzo[*h*][1,3]dioxolo[4,5-*b*]acridine-10, 11-diones (**4a**) was used as a model reaction under a variety of different conditions. The effects of solvents and catalysts were evaluated for this reaction, and the results are summarized in Table 1. It was found that when the reaction was carried out in EtOH without any catalyst the yield of product was low (Table 1, entry 1). DMF as solvent provided higher yields than those using other organic solvents (CH_3CN, $CHCl_3$, and toluene) (Table 1, entry 5 *vs* entries 2−4). To improve the yields, we examined this reaction using different catalysts. Some proton acids can catalyze this reaction with moderate yields. The best result was obtained when γ-Fe_2O_3-HBF_4 was used according to the yield and the reaction time. So γ-Fe_2O_3-HBF_4 was chosen as the catalyst for this reaction. We also evaluated the amount of γ-Fe_2O_3-HBF_4 required for this reaction. The results from Table 1 (entries 11−14) show that 10 mol % γ-Fe_2O_3-HBF_4 at 130 °C in DMF is optimal for the reaction.

< Table 1>

In order to extend the above reaction (Scheme 1) to a library system, various kinds of arylaldehydes **2** (Table 2) were subjected to react with 2-hydroxy-1,4-naphthoquinone **3** and 3,4-methylenedioxyaniline **1** to give the corresponding 12-substituted-benzo[*h*] [1,3]dioxolo[4,5-*b*] acridine-10,11-diones, and representative examples are shown in Table 2. All of **2** gave the expected products in high yields, either bearing electron-withdrawing groups (such as halide and nitro) or electron-donating groups (such as alkyl group) under the same reaction condition. Therefore, we conclude that the electronic nature of substituteds of the aromatic aldehydes had no significant effect on the reaction. Even the heterocyclic aldehydes could be used in this reaction (Table 2, entries 16-17). In addition, an aliphatic aldehyde (Table 2, entry 18) also showed high reactivity under this standard condition providing corresponding 12-methyl-5,10-dihydro-benzo[*i*][1,3]dioxolo[4,5-*b*]acridine-6,11 dione in a good yield of 72%. The structure of the *ortho*-quinone structures **4** is in full agreement with IR, ^{1}H NMR, ^{13}C NMR, and elemental analysis as illustrated below for a representative example (compound **4a**). Compound **4a** exhibited characteristic IR stretching frequencies in the 1678 cm^{-1} regions for C=O. In its ^{1}HNMR spectrum, H-6 and H-9 occur as doublets, respectively, at 8.82 (J = 8.0 Hz) and 8.00 (J = 7.6 Hz) ppm. The H-6 occur about at 9 ppm, more downfield than expected of aromatic protons. This is explicable by the close proximity of these protons to the lone pairs of the neighbouring nitrogens and the consequent anisotropic and van de Waals deshielding. ^{13}C NMR gave two very close carbonyl resonances at δ 180.1 and 179.9 ppm, which was the very close chemical shifts for the carbonyl ^{13}C NMR signals suggested an *ortho*-quinone structure. The molecular formula of all the synthesized compounds was confirmed by element analysis. The purity of the compounds was ascertained by HPLC and were found to be >97% pure.

< Table 2>

The formation of isomeric systems **(***ortho*- and *para*-quinone units**)** is possible in the reaction. So,

we considered it desirable to obtain independent chemical evidence for the presence of *ortho*- or *para*-quinone units in **4**. To this end, we reacted **4e** with *o*-phenylenediamine for 30 min under solvent-free conditions, affording compound **5** in 99% yield, confirming the *ortho*-quinone structure (Scheme 3). The structure of **5** was fully characterized by spectroscopic data and elemental analysis, The H-1 and H-4 occur as a multiplet at 9.25-9.41 ppm, more downfield than expected of aromatic protons. This is explicable by the close proximity of these protons to the lone pairs of the neighbouring nitrogens and the consequent anisotropic and van de Waals deshielding. The lack of any carbonyl signal in ^{13} C NMR spectrum of **5**, and the fact that **5** is formed by the reaction of one molecule of **4e** with one molecule of *o*-phenylenediamine clearly support the structure of **5**, which, in turn, further corroborates the structure of **4** and the regiochemistry of its formation.

< Scheme 3>

A plausible mechanism for the formation of the *ortho*-naphthoquinone is proposed in Scheme 4. We believe that the described transformations proceed *via* the initial formation of respective α, β-unsaturated carbonyl compounds, which undergo nucleophilic attack by the amine. This step is then followed by cyclization and oxidation to yield to product **4**.

< Scheme 4>

The feasibility of repeated use of γ-Fe_2O_3-HBF_4 was also investigated for the reaction of 3,4-methylenedioxyaniline with, 4-chloroaldehyde and 2-hydroxy -1,4-naphthoquinone. We found that this catalyst demonstrated excellent recyclability. The catalyst can be efficiently recovered easily and rapidly from the product by exposure to an external magnet (Figure 10). To remove the residual product, the remaining magnetic nanoparticles were further washed with the EtOH, air-dried and used directly for the next round of reaction without further purification. The recycled catalyst was used

for up to 6 runs with little loss of activity (Table 3).

< Figure 10>

< Table 3>

The biological activities of this series of 12-substituted-benzo[*h*][1,3]dioxolo[4,5-*b*]acridine-10, 11-diones were evaluated by an cytotoxicity assay, which was carried out in a panel of two human tumor cell lines comprising (liver and ovarian) by using the MTT method.[19] The results are summarized in Table 4, and compared to Doxorubicin. It is observed that most of the compounds are significantly cytotoxic. It appears from the data that 3-substitutions of an electron-withdrawing group in the 12-phenyl ring enhances the cytotoxicity as seen in compounds **4o**, **4i** and **4m** for the two cancer cell line. A methyl substituted in the 12-phenyl ring also enhance the cytotoxicity (**4r**). Among the 19 new compounds screened, **4d** has pronounced activity.

< Table 4>

Conclusion

In summary, we have synthesized the first γ-Fe_2O_3-HBF_4 for use as a magnetically heterogeneous nanocatalyst. The catalyst is easily synthesized and can catalyze the synthesis of 12-substituted-benzo[*h*][1,3]dioxolo[4,5-*b*]acridine-10,11-diones with good to high yields. The characteristic aspects of this catalyst are rapid, simple and efficient separation by using an appropriate external magnet, which minimizes the loss of catalyst during separation and reusable for several times with little loss of activity. In addition, this method is simple and convenient to prepare a wide range of *ortho*-quinone derivatives in a single-step operation which are found to possess interesting antitumor properties.

Experimental Section

General

IR spectra were determined on FTS-40 infrared spectrometer. NMR spectra were determined on

Bruker AV-400 spectrometer at room temperature using TMS as internal standard. Chemical shifts (d) are given in ppm and coupling constants (*J*) in Hz. Elemental analysis was performed by a Vario-III elemental analyzer. Melting points were determined on a XT-4 binocular microscope and were uncorrected. Commercially available reagents were used throughout without further purification unless otherwise stated.

Preparation of large-scale the magnetic γ-Fe_2O_3 nanoparticles

$FeCl_2 \cdot 4H_2O$ (9.25 mmol) and $FeCl_3 \cdot 6H_2O$ (15.8 mmol) were dissolved in deionized water (150 mL) under Ar atmosphere at room temperature. A NH_4OH solution (25%, 50 mL) was then added dropwise to the stirring mixture at room temperature to reach the reaction pH to 11. The resulting black dispersion was continuously stirred for 1 h at room temperature and then heated to reflux for 1 h to yield a brown dispersion. The magnetic nanoparticles were then purified by a repeated centrifugation, decantation, and redispersion cycle 3 times. The as-synthesized sample was heated at 2 $^{\circ}C\ min^{-1}$ up to 200 $^{\circ}C$ and then kept in the furnace for 3 h to give a reddish-brown powder.

Synthesis of γ-Fe_2O_3-HBF_4

To a suspension of γ-Fe_2O_3 (16 g) in Et_2O (500 mL), 40% aq. HBF_4 (1.1 g, 5 mmol) was added. The mixture was irradiated in the ultrasonic bath for 180 min at room temperature. The mixture was concentrated and the residue dried under vacuum at 100 °C for 72 h to afford γ-Fe_2O_3-HBF_4 (0.32 mmol/g).

Ion-exchange pH analysis

To an aqueous solution of NaCl (1 M, 25 ml) with a primary pH of 5.93, the catalyst (500 mg) was added and the resulting mixture was stirred for 2 h, after which the pH of the solution decreased to 2.19. This is equal to a loading of 0.32 mmol $HBF_4\ g^{-1}$.

General procedure for the synthesis of compounds 4

To a mixture of 3,4-methylenedioxyaniline (1 mmol), aldehydes (1 mmol), 2-hydroxy-1,4-naphthoquinone (1 mmol) and DMF (10 mL), γ-Fe_2O_3-HBF_4 (0.1 mmol) was added. The mixture was stirred at 130 °C for an appropriate time (Table 2). After completion of the reaction, the catalyst was separated with the aid of an external magnet. Then the reaction mixture was cooled to room temperature. The precipitate was collected by filtration to afford the pure product **4**.

12-(4-Chlorophenyl)-benzo[*h*][1,3]dioxolo[4,5-*b*]acridine-10,11-dione (**4a**): Orange powder, m.p. >300 ^{o}C; IR (KBr): *v* 3060, 2899, 1678, 1537, 1460, 1435, 1261, 1212, 1169, 1161, 1028, 944, 855,772, 556 cm^{-1}; ^{1}H NMR (400 MHz, DMSO-d_6) *δ*: 8.82 (d, 1H, *J* = 8.0 Hz, ArH), 8.00 (d, 1H, *J* = 7.6 Hz, ArH), 7.88 (t, 1H, *J* = 7.6 Hz, ArH), 7.64 (t, 1H, *J* = 7.6 Hz, ArH), 7.57 (d, 2H, *J* = 7.6 Hz, ArH), 7.51 (s, 1H, ArH), 7.26 (d, 2H, *J* = 7.6 Hz, ArH), 6.52 (s, 1H, ArH), 6.23 (s, 2H, OCH_2O); ^{13}C NMR (100 MHz, DMSO-d_6) *δ*: 180.1, 179.9, 153.9, 150.1, 149.7, 149.6, 148.6, 137.7, 136.5, 135.9, 133.1, 132.3, 131.2, 130.5, 128.9, 128.5, 126.6, 124.8, 122.0, 106.1, 103.5,102.1; Anal. Calc. for $C_{24}H_{12}ClNO_4$: C 69.66, H 2.92, N 3.38; found: C 69.72., H 2.82, N 3.29.

12-(2-Chlorophenyl)-benzo[*h*][1,3]dioxolo[4,5-*b*]acridine-10,11-dione (**4b**): Orange powder, m.p. >300 ^{o}C; IR (KBr): *v* 3062, 2914, 1679, 1536, 1459, 1434, 1260, 1210, 1167, 1028, 944, 854, 771, 551 cm^{-1}; ^{1}H NMR (400 MHz, DMSO-d_6) *δ*: 8.83 (d, 1H, *J* = 7.6 Hz, ArH), 8.01 (d, 1H, *J* = 8.0 Hz, ArH), 7.93-7.88 (m, 1H, ArH), 7.67-7.47 (m, 6H, ArH), 7.20 (dd, 1H, *J* = 1.6, 7.6 Hz, ArH), 6.36 (s, 1H, ArH), 6.27 (s, 2H, OCH_2O); ^{13}C NMR (100 MHz, DMSO-d_6) *δ*: 179.4, 179.3, 154.1, 150.1, 150.0, 148.7, 147.8, 137.5, 136.6, 135.9, 132.3, 131.9, 131.3, 130.2, 130.0, 129.7, 128.7, 128.0, 126.5, 124.4, 121.8, 106.2, 103.7,101.3; Anal. Calc. for $C_{24}H_{12}ClNO_4$: C 69.66, H 2.92, N 3.38; found: C 69.60., H 3.02, N 3.33.

12-(4-Fluorophenyl)-benzo[*h*][1,3]dioxolo[4,5-*b*]acridine-10,11-dione (**4c**): Orange powder, m.p. >300 ^{o}C; IR (KBr): *v* 3067, 2902, 1681, 1608, 1538, 1462, 1434, 1260, 1225, 1207, 1170, 1031, 940,

861, 846, 557 cm^{-1}; ^{1}H NMR (400 MHz, DMSO-d_6) δ: 8.82 (d, 1H, J = 7.6 Hz, ArH), 8.01 (d, 1H, J = 7.6 Hz, ArH), 7.89 (t, 1H, J = 7.2 Hz, ArH), 7.55 (s, 1H, ArH), 7.38-7.26 (m, 4H, ArH), 6.53 (s, 1H, ArH), 6.25 (s, 2H, OCH_2O); ^{13}C NMR (100 MHz, DMSO-d_6) δ: 179.9, 179.8, 163.5, 153.8, 150.1, 149.9, 149.6, 148.4, 137.6, 135.8, 133.8, 132.3, 131.2, 130.7, 130.6, 128.5, 126.5, 125.0, 122.2, 115.9, 115.7, 106.1, 103.6, 102.1; Anal. Calc. for $C_{24}H_{12}FNO_4$: C 72.54, H 3.04, N 3.52; found: C 72.58, H 3.00, N 3.61.

12-(2-Fluorophenyl)-benzo[*h*][1,3]dioxolo[4,5-*b*]acridine-10,11-dione (**4d**): Orange powder, m.p. 280-281 ^{o}C; IR (KBr): ν 3069, 2921, 1682, 1541, 1462, 1435, 1259, 1207, 1170, 1033, 942, 861, 769 cm^{-1}; ^{1}H NMR (400 MHz, DMSO-d_6) δ: 8.83 (d, 1H, J = 7.6 Hz, ArH), 8.02 (d, 1H, J = 7.6 Hz, ArH), 7.89 (t, 1H, J = 7.6 Hz, ArH), 7.65 (t, 1H, J = 7.6 Hz, ArH), 7.59-7.55 (m, 2H, ArH), 7.39-7.35 (m, 2H, ArH), 7.24 (t, 1H, J = 7.2 Hz, ArH), 6.50 (s, 1H, ArH), 6.25 (s, 2H, OCH_2O); ^{13}C NMR (100 MHz, DMSO-d_6) δ: 179.9, 179.6, 169.1, 154.1, 150.2, 150.0, 148.7, 144.7, 137.6, 135.9, 132.3, 131.2, 130.9, 130.8, 130.6, 130.5, 128.6, 125.0, 124.9, 116.0, 115.8, 106.2, 103.6, 101.5; Anal. Calc. for $C_{24}H_{12}FNO_4$: C 72.54, H 3.04, N 3.52; found: C 72.58, H 3.00, N 3.61.

12-(4-Nitrophenyl)-benzo[*h*][1,3]dioxolo[4,5-*b*]acridine-10,11-dione (**4e**): Yellow powder, m.p. 299-300 ^{o}C; IR (KBr): ν 3057, 2914, 1682, 1593, 1540, 1520, 1462, 1435, 1352, 1258, 1166, 1036, 974, 859, 770, 555 cm^{-1}; ^{1}H NMR (400 MHz, DMSO-d_6) δ: 8.83 (d, 1H, J = 7.6 Hz, ArH), 8.38 (d, 2H, J = 8.0 Hz, ArH), 8.02 (d, 1H, J = 7.6 Hz, ArH), 7.90 (t, 1H, J = 7.6 Hz, ArH), 7.65 (t, 1H, J = 7.6 Hz, ArH), 7.55-7.53 (m, 3H, ArH), 6.50 (s, 1H, ArH), 6.25 (s, 2H, OCH_2O); ^{13}C NMR (100 MHz, DMSO-d_6) δ: 179.8, 179.6, 154.0, 150.1, 149.9, 148.7, 148.6, 147.2, 145.2, 137.6, 135.9, 132.4, 131.3, 130.1, 128.6, 126.6, 124.3, 124.0, 121.7, 106.2, 103.6, 101.9; MS (ESI): m/z 425 $[M+H]^{+}$; Anal. Calc. for $C_{24}H_{12}N_2O_6$: C 67.93, H 2.85, N 6.60; found: C 68.01, H 2.81, N 6.57.

12-(4-Methoxyphenyl)-benzo[*h*][1,3]dioxolo[4,5-*b*]acridine-10,11-dione (**4f**): Orange red powder, m.p. >300 ^{o}C; IR (KBr): *v* 3066, 2957, 2838, 1679, 1611, 1536, 1460, 1434, 1260, 1250, 1167, 1028, 943, 852, 771, 559 cm^{-1}; ^{1}H NMR (400 MHz, DMSO-d_6) δ: 8.81 (d, 1H, *J* = 8.0 Hz, ArH), 7.99 (d, 1H, *J* = 7.6 Hz, ArH), 7.88 (t, 1H, *J* = 7.6 Hz, ArH), 7.51 (s, 1H, ArH), 7.18-7.07 (m, 4H, ArH), 6.59 (s, 1H, ArH), 6.24 (s, 2H, OCH_2O), 3.86 (s, 3H, OCH_3); ^{13}C NMR (100 MHz, DMSO-d_6) δ: 180.2, 180.0, 159.3, 153.6, 151.1, 150.1, 149.4, 148.4, 137.7, 135.8, 132.2, 131.1, 130.0, 129.5, 128.5, 126.6, 125.3, 122.3, 114.3, 106.0, 103.5, 102.3, 55.6; MS (ESI): m/z 410 $[M+H]^+$; Anal. Calc. for $C_{25}H_{15}NO_5$: C 73.35, H 3.69, N 3.42; found: C 73.42, H 3.62, N 3.32.

12-(2-Methoxyphenyl)-benzo[*h*][1,3]dioxolo[4,5-*b*]acridine-10,11-dione (**4g**): Orange red powder, m.p. >300 ^{o}C; IR (KBr): *v* 3061, 2953, 2841, 1681, 1536, 1463, 1434, 1257, 1237, 1166,1035, 945, 756 cm^{-1}; ^{1}H NMR (400 MHz, DMSO-d_6) δ: 8.81 (d, 1H, *J* = 8.0 Hz, ArH), 7.99 (d, 1H, *J* = 7.6 Hz, ArH), 7.89 (t, 1H, *J* = 7.6 Hz, ArH), 7.64 (t, 1H, *J* = 7.6 Hz, ArH), 7.52 (s, 1H, ArH), 7.50-7.47 (m, 1H, ArH), 7.19 (d, 1H, *J* = 8.4 Hz, ArH), 7.10-7.00 (m, 2H, ArH), 6.46 (s, 1H, ArH), 6.24 (s, 2H, OCH_2O), 3.81 (s, 3H, OCH_3); ^{13}C NMR (100 MHz, DMSO-d_6) δ: 179.9, 179.8, 156.6, 153.9, 132.2, 131.1, 130.0, 129.3, 128.6, 126.5, 126.3, 125.1, 122.3, 121.1, 111.8, 106.0, 103.5, 102.0, 55.9; Anal. Calc. for $C_{25}H_{15}NO_5$: C 73.35, H 3.69, N 3.42; found: C 73.32, H 3.75, N 3.53.

12-(3-Methoxyphenyl)-benzo[*h*][1,3]dioxolo[4,5-*b*]acridine-10,11-dione (**4h**): Orange powder, m.p. >300 ^{o}C; IR (KBr): *v* 3059, 2921, 1682, 1538, 1462, 1434, 1259, 1231, 1165, 1033, 947, 846, 768 cm^{-1}; ^{1}H NMR (400 MHz, DMSO-d_6) δ: 8.82 (d, 1H, *J* = 8.0 Hz, ArH), 8.00 (d, 1H, *J* = 7.6 Hz, ArH), 7.88 (t, 1H, *J* = 7.6 Hz, ArH), 7.64 (t, 1H, *J* = 7.6 Hz, ArH), 7.50 (s, 1H, ArH), 7.44 (t, 1H, *J* = 7.6 Hz, ArH), 7.06 (d, 1H, *J* = 8.0 Hz, ArH), 6.80 (s, 2H, ArH), 6.55 (s, 1H, ArH), 6.23 (s, 2H, OCH_2O), 3.84 (s, 3H, OCH_3); ^{13}C NMR (100 MHz, DMSO-d_6) δ: 180.1, 180.0, 159.9, 153.8, 150.9, 150.1, 149.5, 148.5, 139.0, 137.8, 135.9, 132.3, 131.1, 130.0, 128.5, 126.6, 125.0, 121.9, 120.8, 114.4, 113.7, 106.0,

103.5, 102.3, 55.7; Anal. Calc. for $C_{25}H_{15}NO_5$: C 73.35, H 3.69, N 3.42; found: C 73.40, H 3.59, N 3.47.

12-(3-Nitrophenyl)-benzo[*h*][1,3]dioxolo[4,5-*b*]acridine-10,11-dione (**4i**): Yellow powder, m.p. >300 ^oC; IR (KBr): *v* 3069, 2917, 1685, 1534, 1462, 1434, 1351, 1258, 1208, 1168, 1031, 945, 862, 741 cm^{-1}; ^1H NMR (400 MHz, DMSO-d_6) δ: 8.84 (d, 1H, *J* = 8.0 Hz, ArH), 8.36 (d, 1H, *J* = 8.0 Hz, ArH), 8.12 (s, 1H, ArH), 8.02 (d, 1H, *J* = 7.6 Hz, ArH), 7.91-7.82 (m, 2H, ArH), 7.72 (d, 1H, *J* = 7.6 Hz, ArH), 7.65 (t, 1H, *J* = 7.2 Hz, ArH),7.55 (s, 1H, ArH), 6.55 (s, 1H, ArH), 6.245 (s, 2H, OCH_2O); ^{13}C NMR (100 MHz, DMSO-d_6) δ: 179.6, 179.5, 153.9, 150.0, 149.9, 148.5, 148.0, 139.5, 137.5, 135.9, 135.4, 132.3, 131.3, 130.5, 128.6, 126.5, 124.6, 123.5, 132.2, 122.1, 117.7, 106.1, 103.6, 102.0; Anal. Calc. for $C_{24}H_{12}N_2O_6$: C 67.93, H 2.85, N 6.60; found: C 67.88, H 2.88, N 6.52.

12-(3,4-dichlorophenyl)-benzo[*h*][1,3]dioxolo[4,5-*b*] acridine-10,11-dione (**4j**): Yellow powder, m.p. >300 ^oC; IR (KBr): *v* 3065, 2922, 1683, 1612, 1537, 1463, 1435, 1260, 1209, 1168, 1028, 943, 853, 768 cm^{-1}; ^1H NMR (400 MHz, DMSO-d_6) δ: 8.80 (d, 1H, *J* = 8.0 Hz, ArH), 8.01 (d, 1H, *J* = 8.0 Hz, ArH), 7.88 (t, 1H, *J* = 7.6 Hz, ArH), 7.79 (d, 1H, *J* = 8.0 Hz, ArH), 7.64 (t, 1H, *J* = 7.6 Hz, ArH), 7.54-7.52 (m, 2H, ArH), 7.25 (dd, 1H, *J* = 2.0, 8.0 Hz, ArH), 6.60 (s, 1H, ArH), 6.26 (s, 2H, OCH_2O); ^{13}C NMR (100 MHz, DMSO-d_6) δ: 176.6, 176.5, 153.9, 149.9, 149.8, 148.5, 147.8, 138.5, 137.5, 135.9, 132.2, 131.7, 131.2, 131.0, 130.5, 129.0, 128.6, 126.5, 124.5, 122.0, 106.1, 103.6, 102.0; Anal. Calc. for $C_{24}H_{11}Cl_2NO_4$: C 64.31, H 2.47, N 3.12; found: C 64.24, H 2.53, N3.19.

12-(2,4-dichlorophenyl)-benzo[*h*][1,3]dioxolo[4,5-*b*] acridine-10,11-dione (**4k**): Yellow powder, m.p. >300 ^oC; IR (KBr): *v* 3060, 2918, 1680, 1538, 1464, 1436, 1260, 1209, 1171, 1033, 943, 855,794 cm^{-1}; ^1H NMR (400 MHz, DMSO-d_6) δ: 8.82 (d, 1H, *J* = 8.0 Hz, ArH), 8.02 (d, 1H, *J* = 7.6 Hz, ArH), 7.90 (t, 1H, *J* = 7.6 Hz, ArH), 7.79 (s, 1H, ArH), 7.65 (t, 1H, *J* = 7.6 Hz, ArH), 7.58-7.54 (m, 2H, ArH), 7.26 (d, 1H, *J* = 8.4 Hz, ArH), 6.470 (s, 1H, ArH), 6.27 (s, 2H, OCH_2O); ^{13}C NMR (100 MHz,

DMSO-d_6) δ: 179.6, 179.5, 154.3, 150.2, 150.1, 148.9, 146.7, 137.5,136.0, 135.7, 134.0, 133.1, 132.3, 131.4, 131.3, 129.4, 128.7, 128.2, 126.5, 124.3, 121.8, 106.3, 103.7, 101.4; Anal. Calc. for $C_{24}H_{11}Cl_2NO_4$: C 64.31, H 2.47, N 3.12; found: C 64.35, H 2.45, N 3.13.

12-(2,5-dimethoxyphenyl)-benzo[*h*][1,3]dioxolo[4,5-*b*]acridine-10,11-dione (**4l**): Orange powder, m.p. >300 ^{o}C; IR (KBr): *v* 3073, 3002, 2961, 2837, 1681, 1670, 1540, 1492, 1463, 1436, 1261, 1228, 1217, 1166, 1039, 1017, 948, 864, 729 cm^{-1}; ^{1}H NMR (400 MHz, DMSO-d_6) δ: 8.83 (d, 1H, *J* = 8.4 Hz, ArH), 8.01 (d, 1H, *J* = 7.2 Hz, ArH), 7.90 (t, 1H, *J* = 7.6 Hz, ArH), 7.64 (t, 1H, *J* = 7.6 Hz, ArH), 7.51 (s, 1H, ArH), 7.13-7.03 (m, 2H, ArH), 6.64 (s, 1H, ArH), 6.54 (s, 1H, ArH), 6.24 (s, 2H, OCH_2O), 3.72 (s, 3H, OCH_3), 3.55 (s, 3H, OCH_3); ^{13}C NMR (100 MHz, DMSO-d_6) δ: 180.2, 180.0, 154.0, 153.9, 150.7, 150.1, 149.6, 148.6, 137.8, 136.0, 132.2, 131.2, 128.6, 127.3, 126.6, 126.0, 125.0, 122.3, 115.5, 114.6, 113.3, 106.0, 103.5, 102.1, 56.6, 56.1; Anal. Calc. for $C_{26}H_{17}NO_6$: C 71.07, H 3.90, N 3.19; found: C 71.23, H 3.87, N 3.21.

12-(3,5-dimethoxyphenyl)-benzo[*h*][1,3]dioxolo[4,5-*b*]acridine-10,11-dione (**4m**): Orange red powder, m.p. >300 ^{o}C; IR (KBr): *v* 3095, 2968, 2844, 1681, 1594, 1536, 1462, 1435, 1259, 1208, 1162, 1029, 935, 860, 768 cm^{-1}; ^{1}H NMR (400 MHz, DMSO-d_6) δ: 8.82 (d, 1H, *J* = 7.2 Hz, ArH), 8.01 (d, 1H, *J* = 8.0 Hz, ArH), 7.91-7.87 (m, 1H, ArH), 7.66-7.63 (m, 1H, ArH), 7.53 (s, 1H, ArH), 6.62 (s, 1H, ArH), 6.37 (d, 1H, *J* = 2.4 Hz, ArH), 6.25 (s, 2H, OCH_2O), 3.75 (s, 6H, $2OCH_3$); ^{13}C NMR (100 MHz, DMSO-d_6) δ: 179.8, 179.6, 160.0, 153.8, 150.7, 150.0, 149.5, 148.3, 139.7, 137.7, 135.8, 132.3, 131.1, 128.5, 126.5, 124.8, 121.9, 106.6, 106.0, 103.5,102.2, 99.8, 55.8; Anal. Calc. for $C_{26}H_{17}NO_6$: C 71.07, H 3.90, N 3.19; found: C 71.15, H 3.96, N 3.16.

12-(3-Bromo-4-methoxyphenyl)-benzo[*h*][1,3]dioxolo[4,5-*b*]acridine-10,11-dione (**4n**): Orange powder, m.p. >300 ^{o}C; IR (KBr): *v* 3059, 2061, 1682, 1611, 1536, 1461, 1435, 1287, 1257, 1241, 1206, 1169, 1030, 941, 767 cm^{-1}; ^{1}H NMR (400 MHz, DMSO-d_6) δ: 8.81 (d, 1H, *J* = 8.0 Hz, ArH), 8.00 (d,

1H, *J* = 8.0 Hz, ArH), 7.88 (t, 1H, *J* = 7.2 Hz, ArH), 7.64 (t, 1H, *J* = 7.2 Hz, ArH), 7.53-7.45 (m, 2H, ArH), 7.26-7.223 (m, 2H, ArH), 6.60 (s, 1H, ArH), 6.24 (s, 2H, OCH_2O), 3.97 (s, 3H, OCH_3); ^{13}C NMR (100 MHz, DMSO-d_6) δ: 180.2, 180.1, 155.6, 153.8, 149.7, 149.3, 148.6, 137.7, 135.9, 132.9, 132.2, 131.1, 131.0, 129.4, 129.3, 126.6, 125.9, 125.2, 122.2, 113.2, 111.2, 106.1, 103.5, 102.2, 56.9; Anal. Calc. for $C_{25}H_{14}BrNO_5$: C 61.49, H 2.89, N 2.87; found: C 61.55, H 3.00, N 2.81.

12-(3-Fluoro-4-methoxyphenyl)-benzo[*h*][1,3]dioxolo[4,5-*b*]acridine-10,11-dione (**4o**): Orange red powder, m.p. >300 ^oC; IR (KBr): *v* 3063, 2920, 2851, 1682, 1538, 1464, 1434, 1321, 1259, 1211, 1166, 1034, 940, 854, 760 cm^{-1}; ^1H NMR (400 MHz, DMSO-d_6) δ: 8.80 (d, 1H, *J* = 8.0 Hz, ArH), 8.00 (d, 1H, *J* = 7.6 Hz, ArH), 7.88 (t, 1H, *J* = 8.0 Hz, ArH), 7.64 (t, 1H, *J* = 7.6 Hz, ArH), 7.52 (s, 1H, ArH), 7.31 (t, 1H, *J* = 8.0 Hz, ArH), 7.13 (d, 1H, *J* = 11.2 Hz, ArH), 7.00 (d, 1H, *J* = 8.0 Hz, ArH), 6.63 (s, 1H, ArH), 6.25 (s, 2H, OCH_2O), 3.95 (s, 3H, OCH_3); ^{13}C NMR (100 MHz, DMSO-d_6) δ: 179.9, 179.8, 167.4, 153.7, 150.7, 149.9, 149.6, 148.4, 147.2, 137.6, 135.8, 132.2, 131.2, 128.5, 126.5, 125.1, 125.0, 122.3, 116.7, 116.5, 114.3, 106.0, 103.6, 102.2, 56.5; Anal. Calc. for $C_{25}H_{14}FNO_5$: C 70.26, H 3.30, N 3.28; found: C 70.33, H 3.25, N 3.24.

12-((furan-2-yl))-benzo[*h*][1,3]dioxolo[4,5-*b*]acridine-10,11-dione (**4p**): Orange red powder, m.p. >300 ^oC; IR (KBr): *v* 3060, 2953, 1679, 1595, 1535, 1460, 1433, 1261, 1225, 1166, 1030, 945, 771, 592 cm^{-1}; ^1H NMR (400 MHz, DMSO-d_6) δ: 8.76 (d, 1H, *J* = 7.6 Hz, ArH), 8.00 (d, 1H, *J* = 8.0 Hz, ArH), 7.91 (s, 1H, ArH), 7.87 (t, 1H, *J* = 7.6 Hz, ArH), 7.64 (t, 1H, *J* = 7.6 Hz, ArH), 7.52 (s, 1H, ArH), 7.02 (s, 1H, ArH), 6.75-6.69 (m, 2H, ArH), 6.29 (s, 2H, OCH_2O); ^{13}C NMR (100 MHz, DMSO-d_6) δ: 179.7, 179.6, 154.1, 150.2, 148.8, 147.6, 144.7, 138.5, 137.4, 135.8, 132.3, 131.2, 128.5, 126.4, 124.5, 122.8, 111.9, 111.8, 106.2, 103.7, 101.5; Anal. Calc. for $C_{22}H_{11}NO_5$: C 71.55, H 3.00, N 3.79; found: C 71.60, H 2.96, N 3.84.

12-(Thiophen-2-yl)-benzo[*h*][1,3]dioxolo[4,5-*b*]acridine-10,11-dione (**4q**): Orange red powder, m.p. >300 ^{o}C; IR (KBr): *v* 3015, 2924, 1679, 1542, 1460, 1434, 1260, 1205, 1160, 1034, 941, 859, 723 cm^{-1}; ^{1}H NMR (400 MHz, DMSO-d_6) δ: 8.82 (d, 1H, *J* = 7.6 Hz, ArH), 8.01 (d, 1H, *J* = 7.6 Hz, ArH), 7.91-7.87 (m, 2H, ArH), 7.88 (t, 1H, *J* = 7.6 Hz, ArH), 7.66-7.62 (m, 1H, ArH), 7.53 (s, 1H, ArH), 7.24 (s, 1H, ArH), 7.03 (s, 1H, ArH), 6.75 (s, 1H, ArH), 6.26 (s, 2H, OCH_2O); ^{13}C NMR (100 MHz, DMSO-d_6) δ: 179.9, 179.7, 154.0, 150.3, 148.5, 147.2, 1444.4, 137.0, 135.9, 132.3, 131.2, 128.5, 127.9, 127.7, 126.6, 126.1, 123.2, 113.5,113.0, 105.9, 103.6,101.8; Anal. Calc. for $C_{22}H_{11}NO_4S$: C 68.56, H 2.88, N 3.63; found: C 68.55, H 2.92, N 3.70.

12-methyl-benzo[*h*][1,3]dioxolo[4,5-*b*]acridine-10,11-dione (**4r**): Orange red powder, m.p. 263-265 ^{o}C; IR (KBr): *v* 3066, 2922, 1679, 1601, 1571, 1501, 1469, 1437, 1253, 1243, 1037, 939,774,721 cm^{-1}; ^{1}H NMR (400 MHz, DMSO-d_6) δ: 8.71 (d, 1H, *J* = 8.0 Hz, ArH), 7.92 (d, 1H, *J* = 6.8 Hz, ArH), 7.76 (t, 1H, *J* = 7.6 Hz, ArH), 7.63 (t, 1H, *J* = 7.6 Hz, ArH), 7.48 (s, 1H, ArH), 6.29 (s, 2H, OCH_2O), 1.22 (s, 3H, CH_3); ^{13}C NMR (100 MHz, DMSO-d_6) δ: 179.1, 178.9, 154.3, 149.2, 148.2, 147.3, 145.4, 137.1, 135.3, 132.4, 131.0, 128.9, 126.5, 125.7, 118.0, 108.9, 104.7,102.0, 24.7; Anal. Calc. for $C_{19}H_{11}NO_4$: C 71.92, H 3.49, N 4.41; found: C 72.02, H 3.44, N 4.37.

Typical procedure for the synthesis of compounds 5

A mixture of 12-(4-Nitrophenyl)-benzo[*h*][1,3]dioxolo [4,5-*b*]acridine-10,11-dione (1 mmol) and *o*-phenylenediamine (1.2 mmol) was heated at 100 °C for an appropriate time and monitored by TLC until the final conversion. The reaction mixture was then cooled to room temperature and diluted with cold water (40 mL). The solid product was collected by filtration and was purified by recrystallization from 95% EtOH to afford the desired pure products **5** as a pale yellow solid.

12-(4-Nitrophenyl)-benzo[*h*][1,3]dioxolo[4,5-*b*] quinoxalo [2,3-*j*]acridine-10,11-dione (**5**): Yellow powder, m.p. >300 ^{o}C; IR (KBr): *v* 3057, 2910, 1512, 1497, 1461, 1439, 1345, 1270, 1213, 1183, 1041,

972, 856, 774, 552 cm^{-1}; ^{1}H NMR (400 MHz, DMSO-d_6) δ: 9.41 (d, 1H, J = 7.6 Hz, ArH), 9.25 (d, 2H, J = 7.6 Hz, ArH), 8.50 (d, 2H, J = 8.4 Hz, ArH), 8.20 (d, 1H, J = 8.4 Hz, ArH), 7.88-7.74 (m, 3H, ArH), 7.65-7.52 (m, 4H, ArH), 7.09 (d, 1H, J = 8.4 Hz, ArH), 6.70 (s, 1H, ArH), 6.16 (s, 2H, OCH_2O); ^{13}C NMR (100 MHz, DMSO-d_6) δ: 152.1, 149.1, 148.8, 147.5, 147.2, 147.0, 143.0, 142.3, 141.0,140.1, 131.8, 130.7, 130.3, 130.0, 129.9, 129.8, 129.1, 128.8, 125.9, 125.4, 120.8, 119.1, 105.7, 102.2, 101.2; Anal. Calc. for $C_{30}H_{16}N_4O_4$: C 72,58, H 3.25, N 11.28; found: C 72.62, H 3.30, N 11.19.

Cytotoxicity assay

Cell viability for all cell lines was determined using the 3-(4,5-Dimethyl-2-thiazolyl)-2,5-diphenyl-2*H*-tetrazolium bromide (MTT) colorimetric assay. Compounds **4a-4r**, **5** were subjected to cytotoxic evaluation against Hela and HepG2 cell lines employing the colorimetric method. Doxorubicin was used as the reference substance.

MTT was dissolved in saline to make the concentration of 5 mg/μL as a stock solution. Cancer cells (3×10^3 cells) suspended in 100 mg/well of MEM medium containing 10% fetal calf serum were seeded onto a 96-well culture plate. After 24 h pre-incubation at 37 ^{o}C in a humidified atmosphere of 5% CO_2/95% air to allow cells attachment, various concentrations of test solution (10 μL/well) as listed in Table 3 were added and then incubated for 48 h under the above condition. At the end of the incubation, 10 μL of tetrazolium reagent was added into each well and then incubated at 37 ^{o}C for 4 h. The supernatant was decanted, and DMSO (100 μL/well) was added to allow formosan solubilization. The optical density (OD) of each well was detected by a microplate reader at 550 nm and for correction at 595 nm. Each determination represents the average means of six replicates. The 50% inhibition concentration (IC_{50}) was determined by curve fitting.

Acknowledgements

We are pleased to acknowledge the financial support from Xinxiang University.

References

1. a) K. Nepali, S. Sharma, M. Sharma, P. M. S. Bedi, K. L. Dhar, *Eur. J. Med. Chem.*, 2014, **77**, 422; (b) K. Nepali, S. Sharma, D. Kumar, A. Budhiraja, K. L. Dhar, *Recent Pat. Anti-Canc.*, 2014, **9**, 303.
2. J. P. Kim, W. G. Kim, H. Koshino, J. Jung, I. Yoo, *Phytochemistry*, 1996. **43**, 425.
3. a) G. Errante, G. L. Motta, C. Lagana, V. Wittebolle, M.-E. Sarciron, R. Barret, *Eur. J. Med. Chem.*, 2006, **41**, 773; b) S. Gafner, J. L. Wolfender, M. Nianga, H. Stoeckli-Evans, K. Hostettmann, *Phytochemistry,* 1996, **42**, 1315.
4. D. O. Moon, Y. H. Choi, N. D. Kim, Y. M. Park, G. Y. Kim, *Int. Immunopharmacol.*, 2007, **7**, 506.
5. V. K. Tando, R. V. Singhb, D. B. Yadava, *Bioorg. Med. Chem. Lett.*, 2004, **14**, 2901.
6. M. Yamashita, M. Kaneko, A. Iida, H. Tokudab, K. Nishimura, *Bioorg. Med. Chem. Lett.*, 2007, **17**, 6417.
7. L. Zhou, W. K. Chan, N. Xu, K. Xiao, H. Luo, K. Q. Luo, D. C. Chang, *Life Sci*., 2008, **83**, 394.
8. X. Chen, J. Ding, Y. M. Ye, J. S. Zhang, *J. Nat. Prod*., 2002, **65**, 1016.
9. M. Dubin, S. H. Fernandez Villamil, A. O. Stoppani, *Medicina,* 2001, **61**, 343.
10. D. Wang, M. Y. Xia, Z. Cui, S. I. Tashiro, S. Onodera, Ikejima, *Biol. Pharm Bull*., 2004, **27**, 1025.
11. J. S. Zhang, J. Ding, Q. M. Tang, M. Li, M. Zhao, L. J. Lu, L. J. Chen, S. T. Yuan, *Bioorg Med Chem. Lett.*, 1999, **9**, 2731.
12. C. Qing, C. Jiang, J. S. Zhang, J. Ding, *Anticancer Drugs*, 2001, **12**, 51.
13. a) H. R. Lu, L. H. Meng, M. Huang, H. Zhu, Z. H. Miao, J. Ding, *Cancer Chemother. Pharmacol.*, 2005, **55**, 286; b) Z. H. Miao, T. Tang, Y. X. Zhang, J. S. Zhang, J. Ding, *Int. J. Cancer,* 2003, **106**, 108.

14. L. H. Meng, J. S. Zhang, J. Ding, *Biochem.Pharmacol.*, 2001, **62**, 733.

15. a) A. H. Lu, E. L. Salabas, F. Schueth, *Angew. Chem. Int. Ed.* 2007, **46**, 1222; b) R. Fu, Xi. Jin, J. Liang, W. Zheng, J. Zhuang, W. Yang, *J. Mater. Chem.*, 2011, **21**, 15352; c) M. Niu, M. Du, Z. Gao, C. Yang, X. Lu, R. Qiao, M. Gao, *Macromol. Rapid Comm.*, 2010, **31**, 1805; d) S. Sobhani, Z. P. Parizi, N. Razavi, *Appl. Catal. A: Gen.*, 2011, **409– 410**, 162.

16. a) A. Megia-Fernandez, M. Ortega-Munoz, J. Lopez-Jaramillo, F. Hernandez- Mateo, F. Santoyo-Gonzalez, *Adv. Synth. Catal.*, 2010, **352**, 3306; b) B. G. Wang, B. C. Ma, Q. O. Wang, W. Wang, *Adv. Synth. Catal.*, 2010, **352**, 2923; c) H. Firouzabadi, N. Iran-poor, M. Gholinejad, J. Hoseini, *Adv. Synth. Catal*., 2011, **353**, 125; d) A. J. Amali, R. K. Rana, *Green Chem.*, 2009, **11**, 1781; e) R. L. Oliveira, P. K. Kiyohara, L. M. Rossi, *Green Chem*., 2010, **12**, 144.

17. a) J.-P. Zhang, W. Fan, J. Ding, B. Jiang, S.-J. Tu, G. Li, *Heterocycles*, 2014, **88**, 1065; b) S. Mahajan, S. Khullar, S. K. Mandal, I. P. Singh, *Chem. Commun.*, 2014, **50**, 10078; c) A. Schatz, Alexander; O. Reiser, W.J. Stark, *Chem. Eur. J.* 2010, **16**, 8950.

18. L. Q. Wu, Z. K. Yin, *Eur. J. Inorg. chem*., 2013, 6156.

19. T. Mosmann, *J. Immunol. Methods*, 1983, **65,** 55.

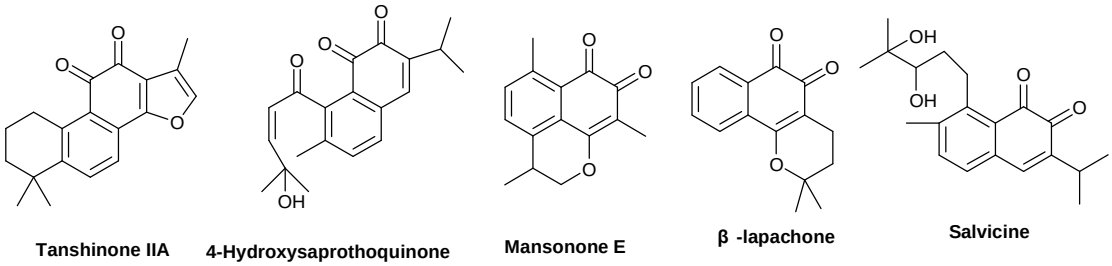

Figure 1. Structures of potent anticancer 1,2-naphthoquinone analogues.

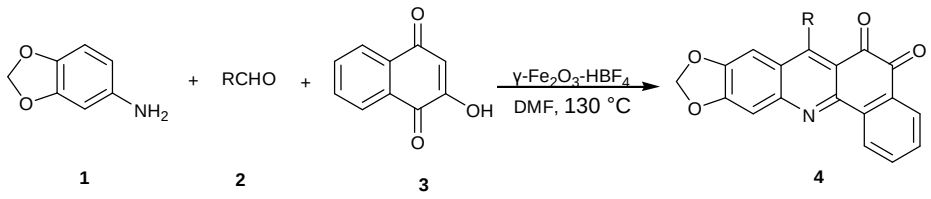

1 2 3 4

Scheme 1. Synthesis of 12-substituted-benzo[*h*] [1,3]dioxolo[4,5-*b*]acridine-10,11-diones catalyzed by γ-Fe_2O_3-HBF_4.

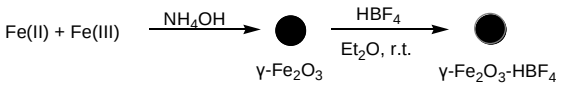

Scheme 2. Synthesis of γ-Fe_2O_3-HBF_4

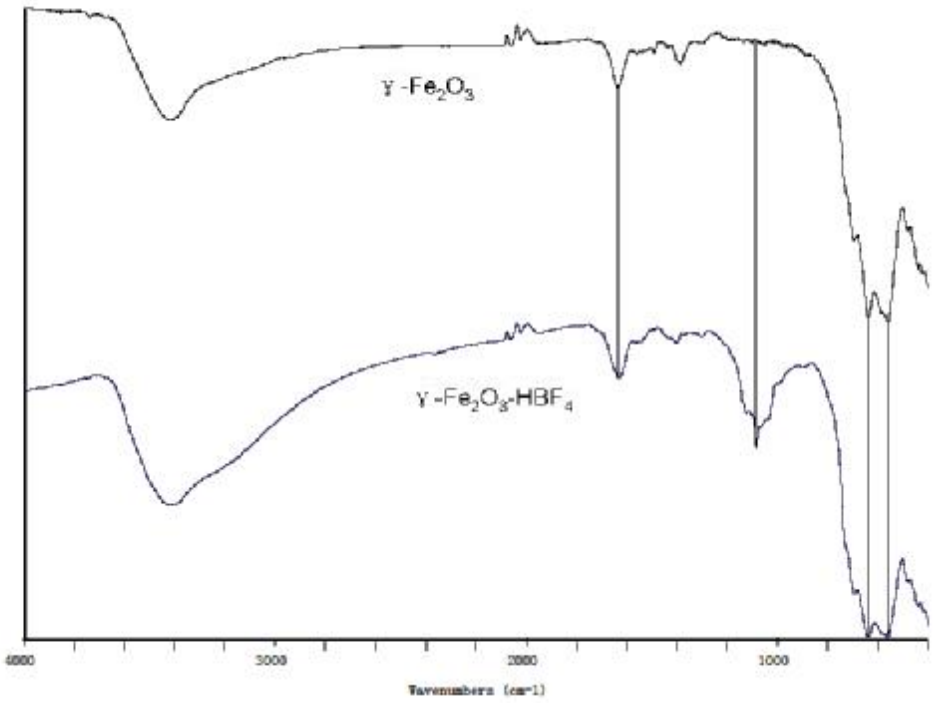

Figure 2. FT-IR spectra of γ-Fe_2O_3 and γ-Fe_2O_3-HBF_4.

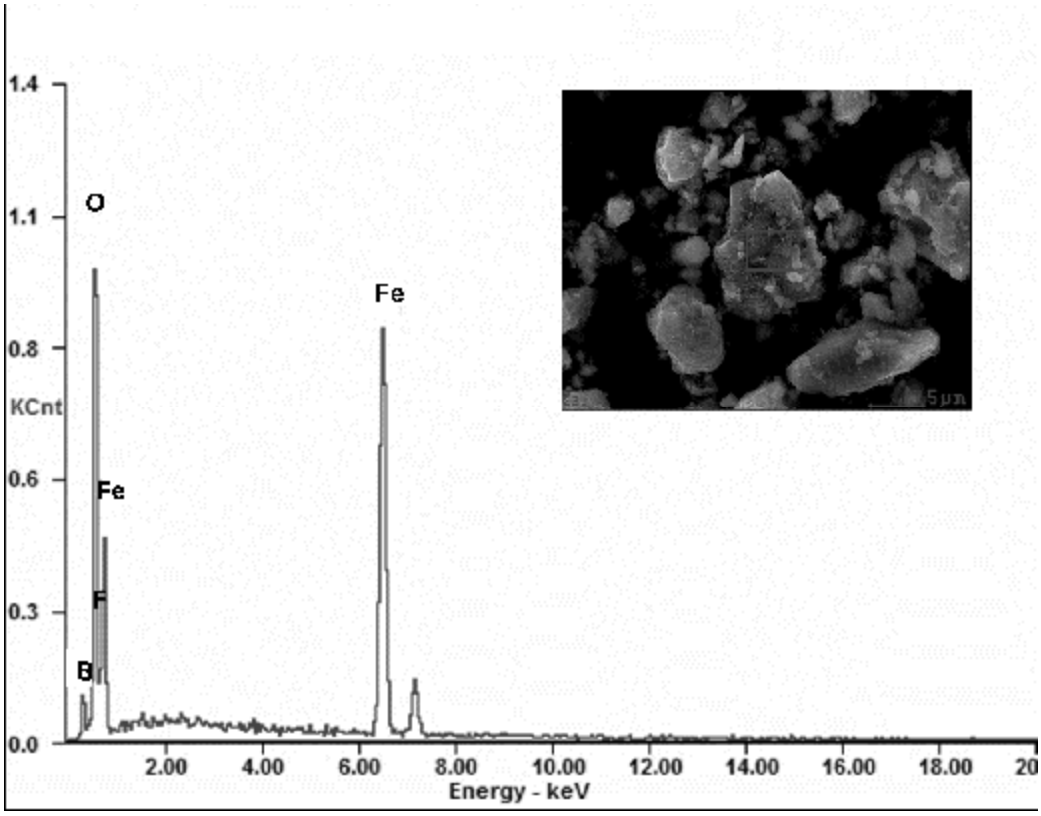

Figure 3. EDS of γ-Fe_2O_3-HBF_4.

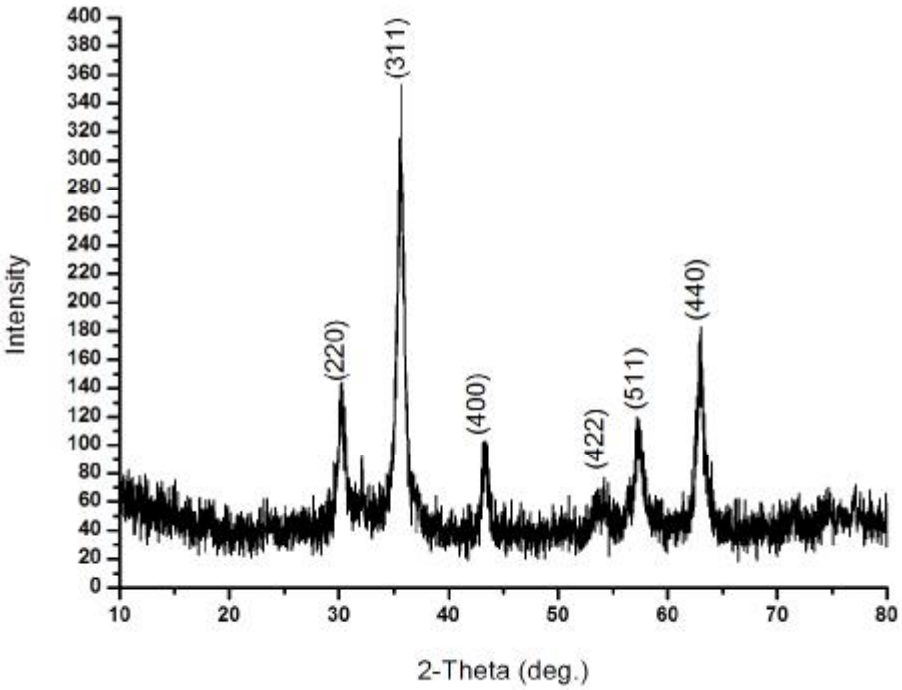

Figure 4a. XRD of γ-Fe_2O_3

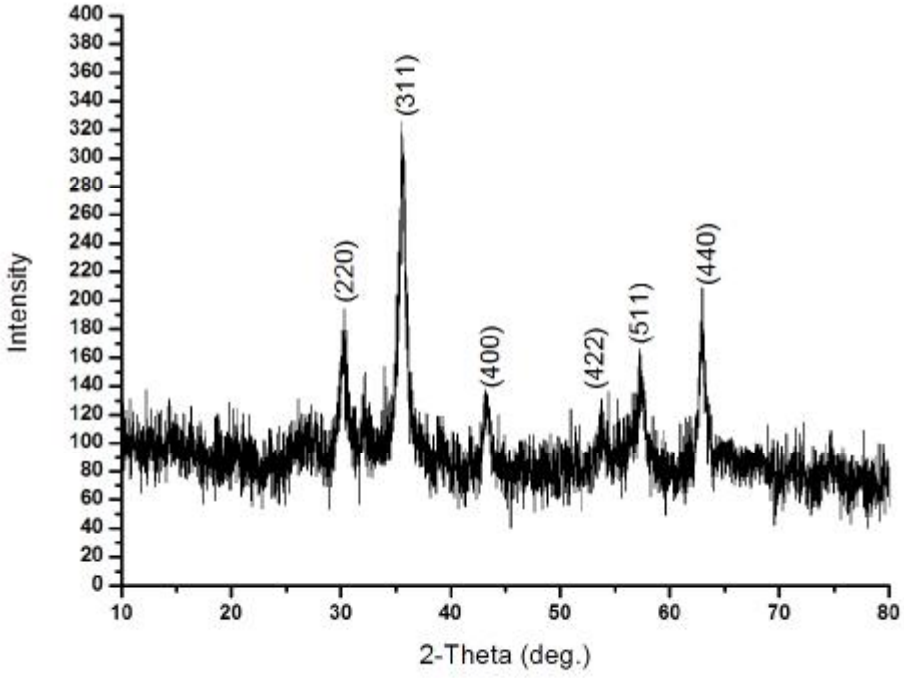

Figure 4b. XRD of γ-Fe_2O_3-HBF_4.

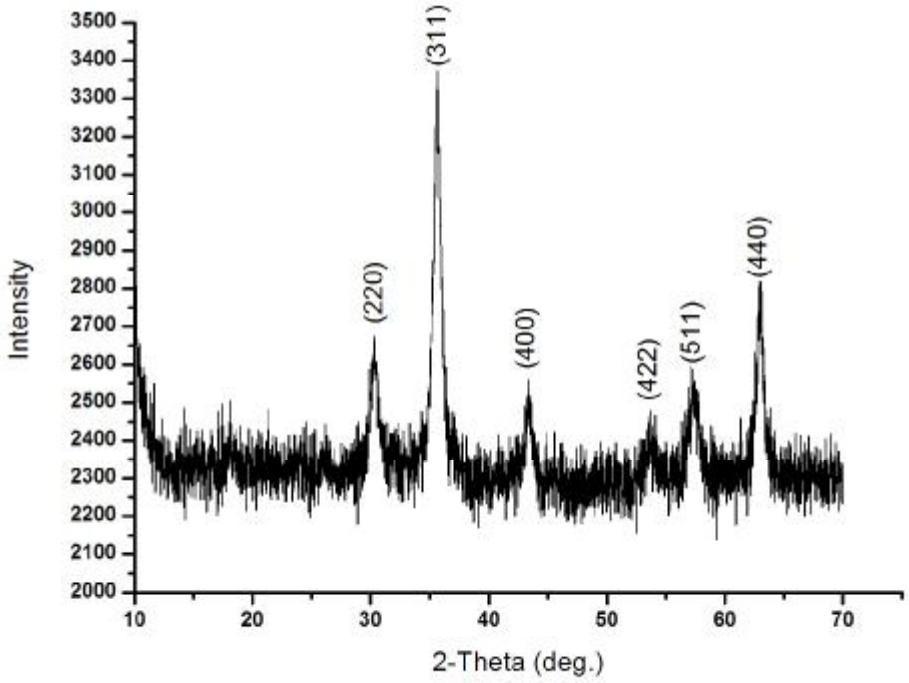

Figure 4c. XRD of γ-Fe_2O_3-HBF_4 heated to 600°C

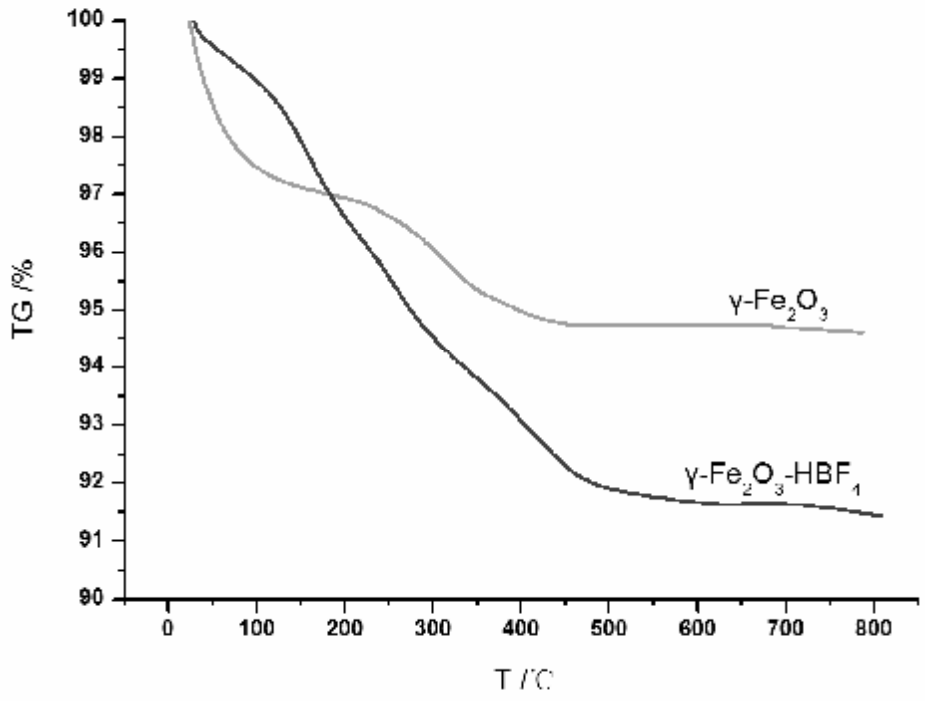

Figure 5. TG analysis for γ-Fe_2O_3 and γ-Fe_2O_3-HBF_4.

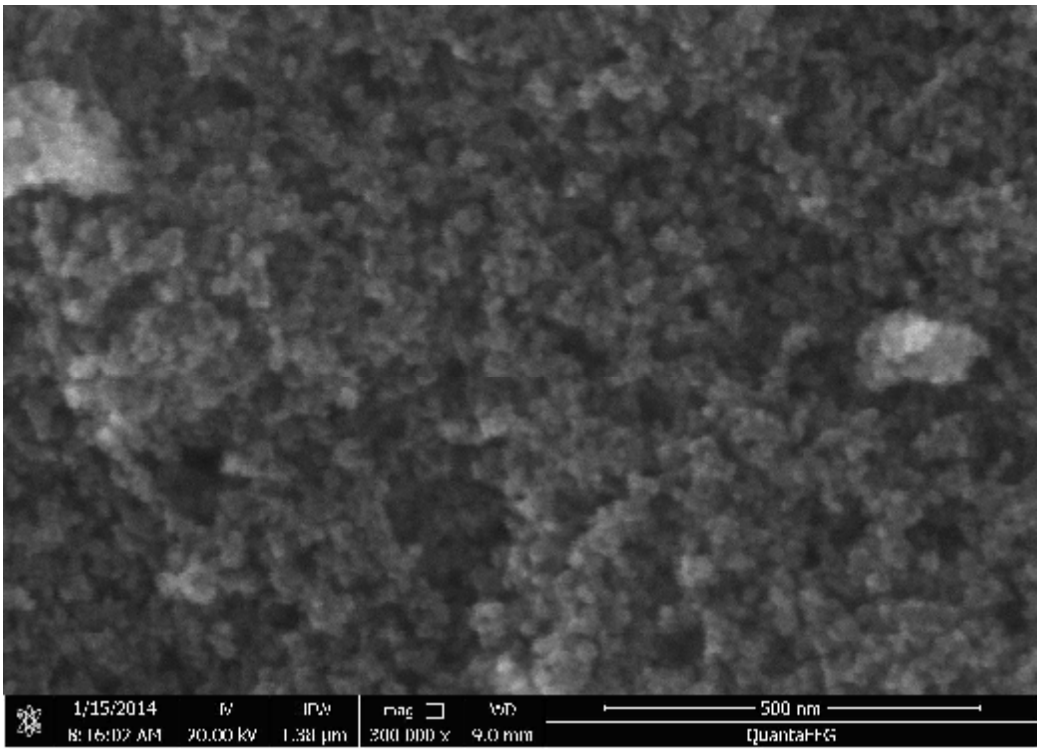

Figure 6a. SEM of γ-Fe_2O_3.

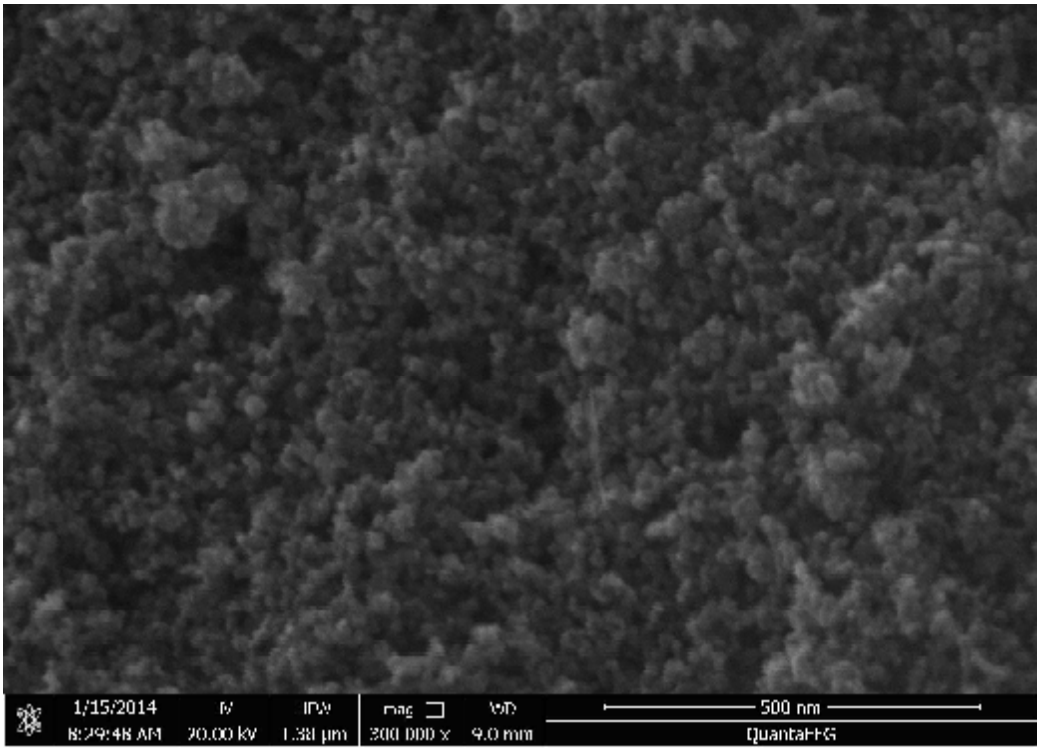

Figure 6b. SEM of γ-Fe_2O_3-HBF_4..

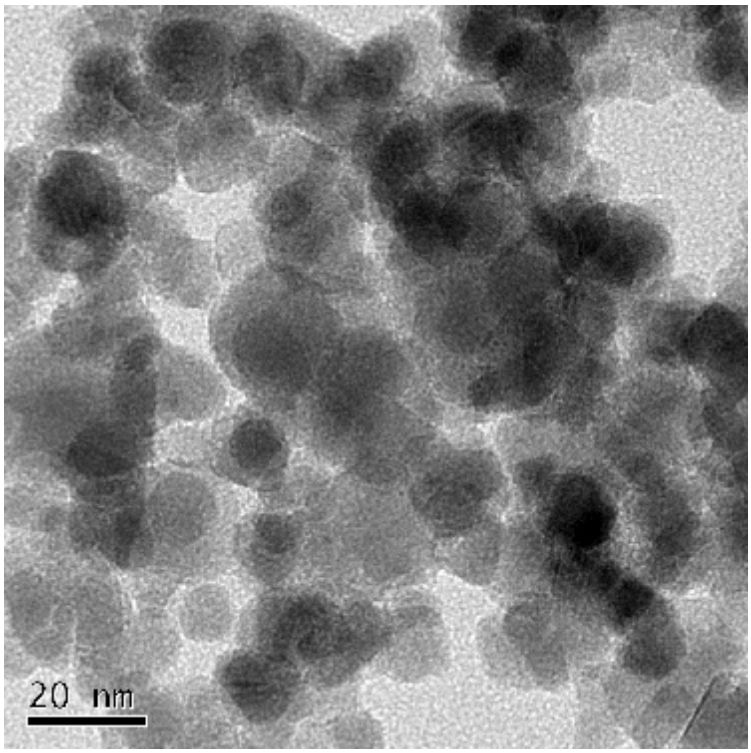

Figure 7a. TEM of γ-Fe_2O_3.

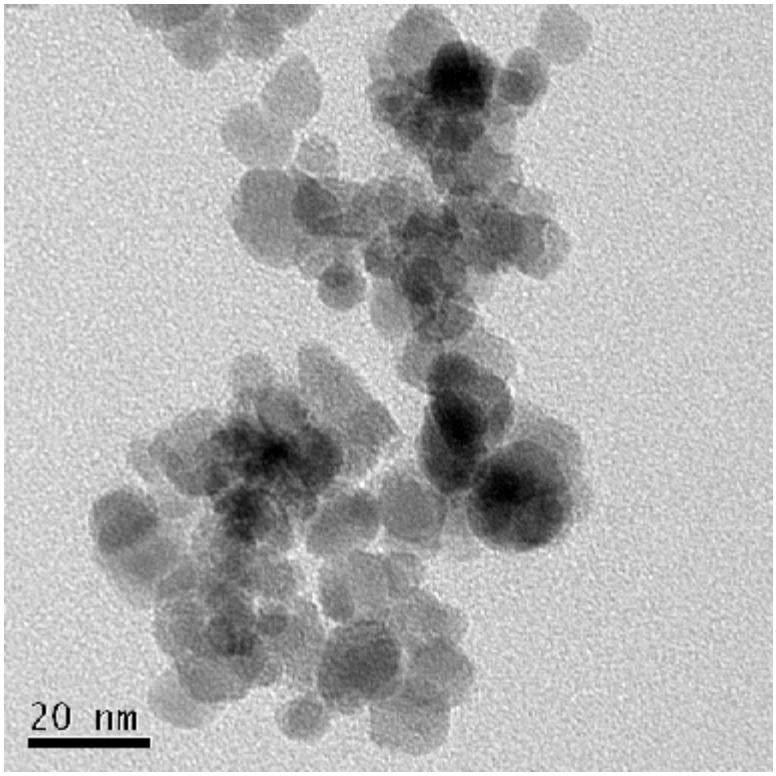

Figure 7b. TEM of γ-Fe_2O_3-HBF_4..

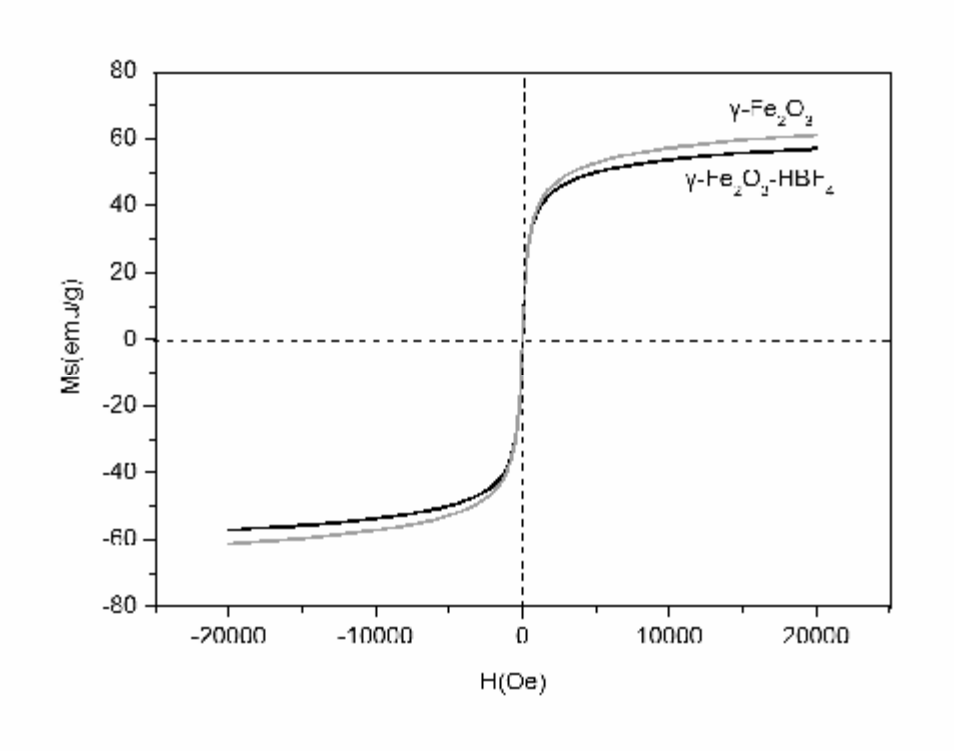

Figure 8. Magnetic curves of γ-Fe_2O_3-HBF_4.

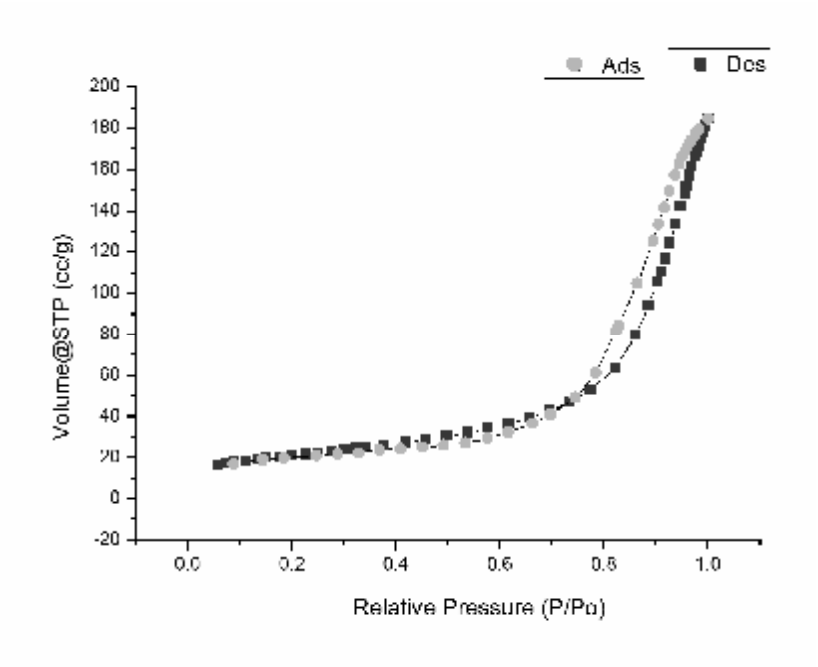

Figure 9a. N_2 adsorption–desorption isotherm of γ-Fe_2O_3

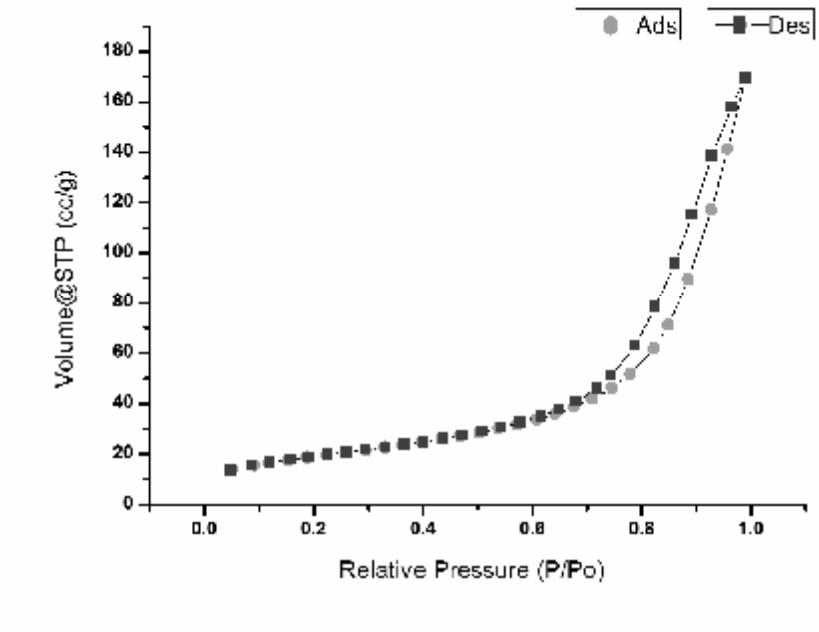

Figure 9b. N_2 adsorption–desorption isotherm of γ-Fe_2O_3-HBF_4

Table 1. Catalyst optimization for the synthesis 12-substituted-benzo[*h*][1,3]dioxolo[4,5-*b*]acridine-10, 11-diones

Entry	Catalyst/ mol%	Solvent	T./ ˚C	Time/ h	Yield/ %[b]
1	-	EtOH	reflux	10	5
2	-	CH_3CN	reflux	5	13
3	-	$CHCl_3$,	reflux	5	6
4	-	toluene	reflux	3	32
5	-	DMF	130	3	54
6	Nano γ-Fe_2O_3 (100)[a]	DMF	130	3	58
7	*p*-TsOH (10)	DMF	130	1	76
8	SiO_2-HBF_4 (10)	DMF	130	1	81
9	$FeCl_3$ (10)	DMF	130	2	59
10	Et_3N (10)	DMF	130	3	67
11	γ-Fe_2O_3-HBF_4 (10)	DMF	130	1	91
12	γ-Fe_2O_3-HBF_4 (5)	DMF	130	1.5	80
13	γ-Fe_2O_3-HBF_4 (15)	DMF	130	1	90
14	γ-Fe_2O_3-HBF_4 (20)	DMF	130	1	91

[a] 100 mg/mmol. [b] Isolated yield.

Table 2. Preparation of 12-substituted-benzo[*h*][1,3] dioxolo[4,5-*b*]acridine-10, 11-diones

Entry	R	Time/ h	Product	Yield/ %[a]
1	4-Cl-C_6H_4	1	**4a**	91
2	2-Cl-C_6H_4	1.5	**4b**	84
3	4-F-C_6H_4	1	**4c**	89
4	2-F-C_6H_4	1.5	**4d**	82
5	4-NO_2-C_6H_4	1	**4e**	92
6	4-MeO-C_6H_4	1	**4f**	90
7	2-MeO-C_6H_4	1.5	**4g**	85
8	3-MeO-C_6H_4	1	**4h**	88
9	3-NO_2-C_6H_4	1	**4i**	84
10	3,4-$(Cl)_2$-C_6H_4	1	**4j**	80
11	2,4-$(Cl)_2$-C_6H_4	1	**4k**	82
12	2,5-$(MeO)_2$-C_6H_3	1.5	**4l**	79
13	3-Br-4-MeO-C_6H_3	1	**4m**	89
14	3,5-$(MeO)_2$-C_6H_3	1.5	**4n**	80
15	3-F-4-MeO-C_6H_3	1	**4o**	82
16	2-Furanyl	1.5	**4p**	86
17	2-Thiophenyl	1.5	**4q**	90
18	Me	1	**4r**	72

[a] Isolated yield.

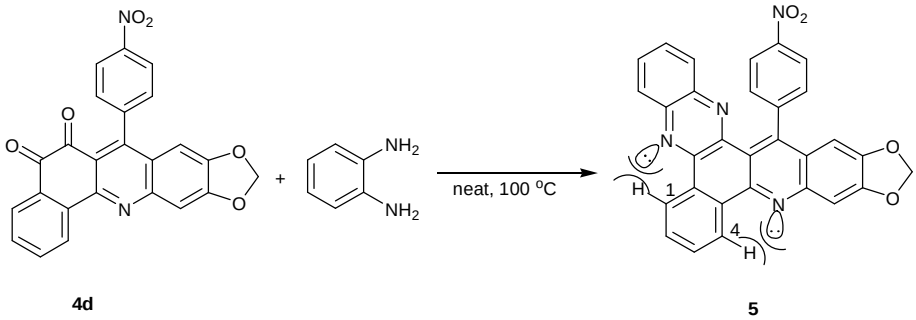

4d 5

Scheme 3. Proof of the *ortho*-quinone structure of **4e**, based on its reaction with *o*-phenylenediamine.

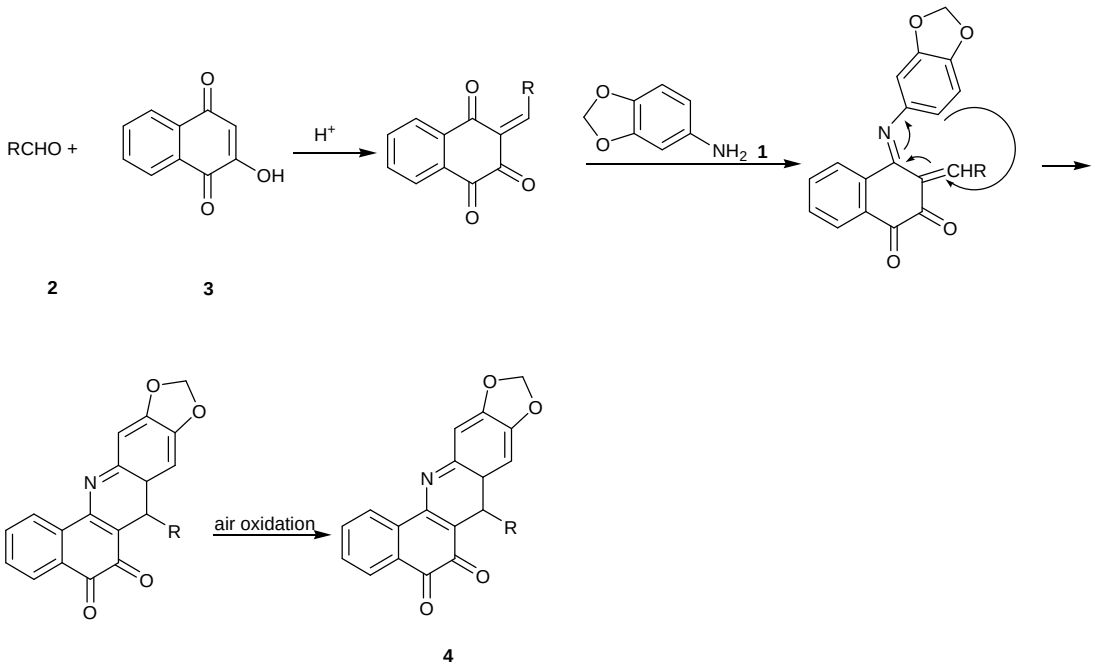

Scheme 4. A plausible mechanistic pathway to explain the γ-Fe_2O_3-HBF_4-catalyzed formation of compounds **4**.

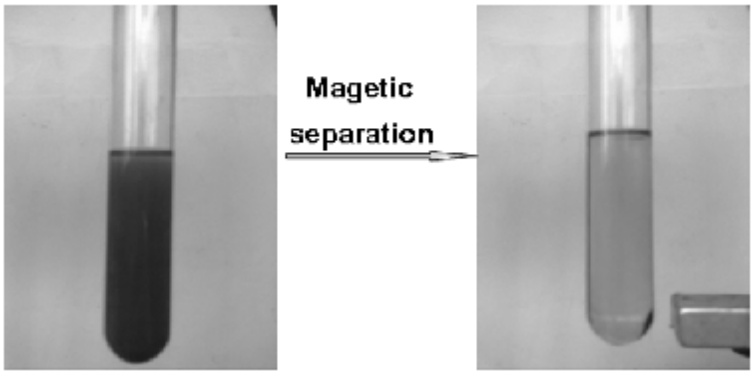

Figure 10. Reaction mixture containing γ-Fe_2O_3-HBF_4 (left), γ-Fe_2O_3-HBF_4 collected using an external magnet after the reaction (right).

Table 3. Recycling experiment for the synthesis of **4a**

Reaction cycles	Element analysis of catalyst / %	The recovery rate of catalyst / %	Loading of HBF_4 / mmol g^{-1} [a]	Yield / %
1	B 0.35, F 2.43, H 0.065	96	0.32	91
2	B 0.32, F 2.24, H 0.057	92	0.29	89
3	B 0.31, F 2.14, H 0.056	90	0.28	87
4	B 0.30, F 2.07, H 0.056	90	0.27	84
5	B 0.29, F 1,99, H 0.055	86	0.26	82
6	B 0.27, F 1.90, H 0.051	85	0.25	79

[a] The amount of HBF_4 loaded on the surface of nano γ-Fe_2O_3 was determined by by ion-exchange pH analysis.

Table 4. Antitumor activities of compounds **4**

Compound	IC_{50} (μM)[a]	
	HepG2	Hela
4a	32.83 ± 5.80	25.05 ± 5.51
4b	>200	>200
4c	>200	>200
4d	4.81 ± 0.22	6.15 ± 0.77
4e	90.89 ± 9.30	119.23 ± 8.87
4f	>200	>200
4g	29.48 ± 0.81	24.74 ± 4.84
4h	>200	>200
4i	13.08 ± 0.50	15.90 ± 4.52
4j	>200	>200
4k	>200	>200
4l	82.31 ± 15.84	69.73 ± 7.04
4m	27.63 ± 1.61	33.80 ± 2.04
4n	>200	>200
4o	5.91 ± 1.10	7.38 ± 3.08
4p	>200	>200
4q	>200	>200
4r	8.59 ± 0.56	6.93 ±0.47
Doxorubicin	2.25 ± 0.44	1.98 ± 0.33

[a] The means of triplicates ± SD